Biosynthesis of benzoxazinoids in rye (*Secale cereale* L.) – where does the story begin?

Monika Rakoczy-Trojanowska[1,*], Elżbieta Różańska[2], Magdalena Święcicka[1,2], Wojciech Burza[1], Beata Bakera[1], Mariusz Kowalczyk[3], Barbara Łotocka[2], Bartosz Szabała[1]

[1] Department of Plant Genetics, Breeding and Biotechnology, Institute of Biology, Warsaw University of Life Sciences (SGGW), Nowoursynowska 166 St., 02-787 Warsaw, Poland

[2] Department of Botany, Institute of Biology, Warsaw University of Life Sciences (SGGW), Nowoursynowska 166 St., 02-787 Warsaw, Poland

[3] Department of Biochemistry and Crop Quality, Institute of Soil Science and Plant Cultivation - State Research Institute, Czartoryskich 8 St., 24-100 Puławy, Poland

*corresponding author: monika_rakoczy_trojanowska@sggw.edu.pl tel. +48-225932150

monika_rakoczy_trojanowska@sggw.edu.pl, elzbieta_rozanska@sggw.edu.pl, magdalena_swiecicka@sggw.edu.pl, wojciech_burza@sggw.edu.pl, beata_bakera@sggw.edu.pl, mkowalczyk@iung.pulawy.pl, barbara_lotocka@sggw.edu.pl, bartosz_szabala@sggw.edu.pl

Running title: Benzoxazinoid synthesis in rye roots.

Date of submission: 05.03.2021

The main manuscript contains 1 table, 5 figures, and 5498 words (start of the introduction to the end of the acknowledgements, excluding materials and methods). There are 3 figures, 2 tables in the Supplementary data.

1

Highlight

The first step benzoxazinoids synthesis occurs in both the above-ground parts and roots of rye plants. Benzoxazinoids can be synthesised *de novo* in roots, independently of plants' photosynthesising parts.

Abstract

According to current opinion, the first step of benzoxazinoids (BXs) synthesis, that is, the conversion of indole-3-glycerol phosphate to indole, occurs exclusively in the photosynthesising parts of plants. However, the results of our previous work and some other studies suggest that this process may also occur in the roots. In this study, we provide evidence that the first step of BXs synthesis does indeed occur in the roots of rye seedlings. We detected *ScBx1* transcripts, BX1 enzyme, and six BXs (2-hydroxy-1,4-benzoxazin-3-one, 2,4-dihydroxy-1,4-benzoxazin-3-one, (2R)-2-O-β-d-glucopyranosyl-4-hydroxy-(2H)-1,4-benzoxazin-3(4H)-one glucoside, 2,4-dihydroxy-7-methoxy-1,4-benzoxazin-3-one, 2,4-dihydroxy-7-methoxy-1,4-benzoxazin-3-one glucoside, and 6-methoxy-2-benzoxazolinone) in the roots developed from seeds deprived of the coleoptile at 2 days after sowing (i.e., roots without contact with aerial parts). In roots regenerated *in vitro*, both *ScBx1* transcripts and BX1 enzyme were detected at a low but still measurable levels. Thus, BXs are able to be synthesised in both the roots and above-ground parts of rye plants.

Keywords: *ScBx1* gene, indole-3-glycerol phosphate lyase, active compounds, roots developing independently, seeds deprived of coleoptile, *in vitro* regeneration

Abbreviations: BSA, bovine serum albumin; BXs, benzoxazinoids; BX1, benzoxazinless1; DIBOA, 2,4-dihydroxy-1,4-benzoxazin-3-one; DIMBOA, 2,4-dihydroxy-7-methoxy-1,4-benzoxazin-3-one; FNR, ferredoxin NADP reductase; GDIBOA, (2R)-2-O-β-d-glucopyranosyl-4-hydroxy-(2H)-1,4-benzoxazin-3(4H)-one glucoside; GDIMBOA, 2,4-dihydroxy-7-methoxy-1,4-benzoxazin-3-one glucoside; GHDMBOA, 2-hydroxy-4,7-dimethoxy-1,4-benzoxazin-3-one glucoside; GTRIBOA, 2,4,7-trihydroxy-1,4-benzoxazin-3-one glucoside; HBOA, 2-hydroxy-1,4-benzoxazin-3-one; IbG, indoxyl β-D-glucoside; L2W, leaves from 2-week-old seedlings; MBOA, 6-methoxy-2-benzoxazolinone; PBS, phosphate-buffered saline; RDC, roots derived from seeds deprived of coleoptiles upon emergence; RIV, roots developed *in vitro*; R2W, roots from 2-week-old seedlings; UGPase, UDP-glucose pyrophosphorylase.

Introduction

Benzoxazinoids (BXs), secondary metabolites synthesised by several species of the Poaceae family, play an important role in biotic and abiotic stress resistance, and in allelopathy. Common rye (*Secale cereale* L.) is among species producing BXs at a particularly high level (Rice et al., 2005, Schulz et al., 2013, Makowska et al., 2015).

There are several steps in BX biosynthesis, the first of which is the conversion of indole-3-glycerol phosphate to indole. Indole is transformed to indolin-1-one and then, after three subsequent mono-oxidations, 2,4-dihydroxy-1,4-benzoxazin-3-one (DIBOA) is synthesised. The glycosylation of DIBOA and 2,4-dihydroxy-7-methoxy-1,4-benzoxazin-3-one (DIMBOA) results in the production of (2R)-2-O-β-d-glucopyranosyl-4-hydroxy-(2H)-1,4-benzoxazin-3(4H)-one glucoside (GDIBOA) and 2,4-dihydroxy-7-methoxy-1,4-benzoxazin-3-one glucoside (GDIMBOA), respectively. The O-methylation of DIBOA and DIMBOA yields 2,4,7-trihydroxy-1,4-benzoxazin-3-one glucoside (GTRIBOA) and 2-hydroxy-4,7-dimethoxy-1,4-benzoxazin-3-one glucoside (GHDMBOA), respectively. Finally, hydroxylation reactions convert GDIBOA to DIBOA and GDIMBOA to DIMBOA (Frey et al., 2009, Meihls et al., 2013, Makowska et al., 2015, Handrick et al., 2016, Wouters et al., 2016).

The first step of BX biosynthesis is controlled by the *Bx1* gene (and its orthologs), which encodes BX1 (benzoxazinless1) with the activity of indole-3-glycerol phosphate lyase (Frey et al., 2009, La Hovary 2011, Bakera et al., 2015, Tanwir et al., 2017).

In rye, besides *ScBx1* (Acc. No. KF636828.1), another gene encoding an indole-3-glycerol phosphate lyase, *ScIgl* (Acc. No. MN120476) takes over the role of *ScBx1* at later developmental stages - between the 42nd and 70th days after germination (Wlazło et al., 2020). In maize, both enzymes can function efficiently *in vitro* (Frey et al., 1997, 2000).

According to current opinion, the conversion of indole-3-glycerol phosphate to indole takes place in the aerial parts of plants, specifically in the chloroplasts (Frey et al., 2009, Meihls et al., 2013, Handrick et al., 2016, Wouters et al., 2016) and not in roots. However, the results of our previous experiments on rye BXs (2-hydroxy-1,4-benzoxazin-3-one - HBOA, DIBOA, GDIBOA, DIMBOA, GDIMBOA and 6-methoxy-2-benzoxazolinone (MBOA)) and expression analyses of BX-related genes indicate that genes encoding indole-3-glycerol phosphate lyases, including *ScBx1*, are expressed both in the aerial parts and roots of 2- to 6-week-old seedlings. This was observed regardless of cultivation conditions; i.e., with or without Berseem clover (Rakoczy-Trojanowska et al., 2020), and at low or normal temperatures (Rakoczy-Trojanowska et al., 2018a, 2018b). Similarly, Tanwir et al., (2017) detected transcripts of six *ScBx* genes including *ScBx1* in the roots of germinating seeds and young seedlings of rye. Transcripts of *Bx1* genes have also been detected in the roots of other cereals, including wheat (Nomura et. al., 2005) and maize (von Rad et al., 2001, van Doan et al., 2020).

Although the results obtained by us and by other groups suggest that the first step of BX synthesis can occur in roots, no previous studies had presented experimental evidence confirming this. Therefore, we decided to test the hypothesis that BXs can be synthesised in roots by conducting detailed analyses of roots developing without contact with aerial plant parts. The results of these experiments and analyses are summarised in this paper.

Materials and methods

Plant material

The following organs of rye (*S. cereale* L.) inbred line L318 (S37), bred in the Department of Plant Genetics, Breeding and Biotechnology, were used in analyses:

- − roots developed from seeds deprived of the coleoptile at 2 days after sowing (RDC)
- − roots developed *in vitro* (RIV)
- − roots (R2W) and leaves (L2W) from 2-week-old seedlings

R2W and L2W were treated as control reference organs (designated as KI and KII, respectively).

To obtain RDC, 180 seeds were sown in Petri dishes on wet filter paper and left to germinate in the dark for 1 – 2 days at 24°C. Out of 180 seeds, 118 germinated. The emerging coleoptiles were cut from the seedlings immediately after emergence and seeds with growing roots were placed back into darkness for another 10 days (Fig. S1; supplementary materials). After this period, RDC were divided into four portions for gene expression, biochemical, immunological, and microscopy analyses.

To produce RIV, an *in vitro* culture was established from mature embryos. Before embryo isolation, seeds were sterilised in a 3% solution of sodium hypochlorite followed by immersion in 70% ethyl alcohol for 3 minutes. The seeds were then washed three times with sterile water (for 15, 10, and 5 minutes). Sterile embryos were placed individually in Petri dishes (Φ10 cm) on a thin layer of modified MS medium (half strength of macro-elements, 30 g/dm^3 sucrose). Roots formed after 2 – 3 weeks were separated from primary explants, cut into fragments of 0.5 – 1 cm, and transferred to Erlenmeyer flasks containing 40 mL of the same medium (0.5 PCV) with Picloram at a concentration of 3 mg/dm^3. The cultures were kept under a 16-h light/8-h dark photoperiod (photosynthetic photon flux density = 50 μmol m^{-2} s^{-1}) at 25°C. After 10 days, secondary roots had formed. The subcultures were done every 7 – 10 days. Roots (hereinafter referred to as RIV, or more generally - organoids) used for gene expression and biochemical analyses were collected between the 14th and 21st day after culture initiation.

The R2W and L2W samples were collected from 2-week-old seedlings. First, seeds were sown in Petri dishes and after 2 days, germinating seeds were transferred to pots containing a 1:1 mixture of perlite and peat substrate (peat mixed with chalk - 6 kg/m^3, MAKRO MIS4 fertiliser - 2 kg/m^3, and MIKRO MIS fertiliser - 100 g/m^3) and cultivated under a 12-h light/12-h dark photoperiod (15°C days, 12°C nights) and 60%–80% relative humidity. This experiment was performed with four biological replicates of 21 plants per replicate.

Immediately after sampling, all collected organs and organoids were frozen in liquid nitrogen, and tissues intended for use in biochemical analyses were lyophilised.

Bioinformatics analysis of BX1

The TargetP 2.0 program (Armenteros et al., 2019) was used to predict the transit peptide. The GRAVY index (average hydrophobicity) was determined according to Kyte and Doolittle (1982).

4

Multiple sequence alignment of different lyases was performed using the Clustal Omega sequence alignment program (www.clustal.,org).

RNA isolation, cDNA synthesis, and quantitative real time-PCR analysis

A GeneMATRIX Universal RNA Purification Kit (version 1.2) (Eurx, Gdańsk, Poland) was used to extract total RNA from RDC, RIV, L2W, and R2W. The isolated RNA was dissolved in 40 μL RNase-free water. The RNA integrity and concentration were measured with a NanoDrop 2000 spectrophotometer. Then, the RNA was treated with Turbo DNase (Thermo Fisher Scientific, Waltham, MA, USA) according to the manufacturer's instructions. The cDNA was transcribed using a High-Capacity cDNA Reverse Transcription kit (Thermo Fisher Scientific) and diluted with RNase-free water.

The transcript levels of *ScBx1* were determined by qRT-PCR. The experiments were carried out in 96-well reaction plates with a Light Cycler 96 Instrument (Roche, Basel, Switzerland). The reaction conditions were as follows: 35 cycles at 95°C for 10 s, 57°C for 10 s, and 72°C for 15 s. *HvAct* (Acc. No. AY145451) served as the internal control, and was chosen based on the geNorm algorithm (https://genorm.cmgg.be). This gene was chosen as the most stable based on preliminary experiments on *ScGADPH* (Acc. No. JQ659189.1) and *Ta54227* (Acc. No. Pr0102692400; Wang et al., 2016). The reaction mixture (total volume 20 μL) consisted of 4 μL cDNA (5 ng/μL), 1 μL each gene-specific primer (5 mM), 4 μL RNase-free water, and 10 μL FastStart Essential DNA Green Master (Roche). The transcript level of the target gene was normalised to that of *HvAct* by the $2^{-\Delta\Delta Ct}$ method (Livak and Schmittgen, 2001). Table 1 shows the sequences of the primers used to amplify *ScBx1* and *HvAct*.

Table 1. Primers used in the qRT-PCR reactions.

Biochemical analysis

Previously published protocols (Święcicka et al., 2020, Wlazło et al., 2020) with some modifications were used to quantify the following BXs: HBOA, GDIBOA, DIBOA, GDIMBOA, DIMBOA, and MBOA. Briefly, plant material (100 mg) was extracted with 70% methanol containing an internal standard (2 μg/ml indoxyl β-D-glucoside; IbG) under the conditions described previously. The obtained extracts were evaporated to dryness under reduced pressure, reconstituted in 1 mL methanol containing 0.1% (v/v) acetic acid, and stored at −20°C. Before analysis, samples were centrifuged for 20 min at 23000 × *g* at 4°C and filtered using Whatmann Mini-Uniprep filtering vials (GE Healthcare, Buckinghamshire, UK) with a regenerated cellulose membrane (0.2-μm pore size).

The BXs were separated on a Waters BEH C18 column (100 × 2.1 mm, 1.7 μm, Waters, Milford, MA, USA) with a linear, 8.5-min gradient from 3% to 15% acetonitrile containing 0.1% (v/v) formic acid (solvent B) in 0.1% formic acid (solvent A). All separations were carried out on a Waters Acquity UPLC system with the column temperature set to 50°C and a flow rate of 0.6 mL/min.

5

The column effluent was redirected into the waste for the first 1.5 minutes of separation, to prevent contamination of the ion source with polar constituents of the sample matrix. The effluent was subsequently directed into a triple quadrupole mass spectrometer (Waters TQD, Manchester, UK) and analysed as described previously. Data acquisition and processing were conducted using Waters MassLynx 4.1 SCN 919 software.

The calibration used seven concentration points, between 0.3 and 35 ng/µL, prepared from standard solutions of DIBOA, DIMBOA, HBOA, GDIMBOA, MBOA, and IbG at 1 mg/mL each. The GDIMBOA curve was used for calibration of GDIBOA. Each concentration point response was calculated as the ratio of the analyte to the IgG peak area. For all investigated compounds, the relationship of concentration vs. response was linear up to 30 ng/µL. The accuracy of the quantification was monitored by injecting quality control samples, consisting of a mixture of all standards at 1, 15, and 30 ng/µL, every ten injections of plant extract samples. Method detection limits were determined from ten separate analyses of 0.3 ng/µL solutions of the calibration standards.

Immunodetection of BX1protein in root and leaf plastids

Preparation of antiserum. Polyclonal antibodies against the peptide VTGPRENVNLRVESL derived from the protein sequence of the rye chloroplast BX1 were raised in a rabbit at Agrisera (Vännäs, Sweden). The antiserum was affinity-purified using the peptide antigen coupled to UltraLink^{TM} Iodoacetyl gel (Thermo Fisher Scientific).

Preimmune serum was affinity-purified using a Protein A IgG Purification Kit (Pierce, Rockford, IL, USA) following the manufacturer's instructions, and was used as a negative control in western blot and histochemical analyses.

Plastid isolation. Plastids were isolated from roots (RDC and R2W) and leaves (L2W). Plant material was ground in a mortar and pestle followed by homogenisation in a Waring blender for 2×10 s in ice-cold buffer (0.33 M sorbitol, 50 mM Tris–HCl, pH 8.0, 2 mM EDTA, 0.1% (w/v) bovine serum albumin (BSA), and 5 mM ascorbic acid). The homogenate was filtered through 100-µm and 40-µm nylon mesh and centrifuged at $200 \times g$ for 2 min and at $2000 \times g$ for 7 min. The resulting pellet of enriched plastids was washed twice in homogenisation medium and then subjected to western blot analysis.

The quality of the isolated plastid fraction was verified by light microscopy and western blotting using compartment marker antibodies directed against ferredoxin NADP reductase (FNR) (Agrisera).

Cytosol isolation. The cytosolic fraction was isolated from roots (RDC and R2W) and leaves (L2W). Plant material was ground in a mortar and pestle and re-suspended in ice-cold homogenisation medium (0.4 M sucrose, 50 mM Tris–HCl, pH 8.0, 5 mM EDTA, 0.1% PVP, 0.1% (w/v) BSA, 5 mM ascorbic acid, and protease inhibitor cocktail). The homogenate was filtered through 100-µm nylon mesh and centrifuged at $12000 \times g$ for 20 min. The resulting supernatant was used as the cytosolic fraction in western blot analyses. The quality of the isolated cytosolic fraction was verified by western

blotting using compartment marker antibodies directed against UDP-glucose pyrophosphorylase (Agrisera).

Preparation of protein extracts. Soluble proteins were extracted from isolated organelles in 50 mM Tris-HCl pH 8.0, 5 mM EDTA, 5% β-mercaptoethanol, and protease inhibitor cocktail. After removal of the soluble fraction, membrane proteins were extracted in the same buffer except that it contained 2% SDS. The protein content was determined using a Modified Lowry Protein Assay Kit (Pierce).

Western blot analysis. Proteins (10 µg) were separated by 10%–12.5% SDS-PAGE and electroblotted onto a 45-µm nitrocellulose membrane (GE Healthcare). Membranes were stained with Ponceau to ensure equal distribution of proteins in each lane. After blocking in a mixture of tris-buffered saline and Polysorbate 20 containing 5% (w/v) non-fat dry milk powder, the membrane was incubated with the primary antibody diluted 1:2000 for 1 h. Following incubation and washing steps, the membrane was incubated with secondary goat anti-rabbit antibody HRP conjugated (Agrisera) for 1 h diluted 1:40000. The protein-antibody complex was detected with the ECL Superbright system (Agrisera) and photographed using the ChemiDoc Imaging System (Bio-Rad, Hercules, CA, USA). Each experiment was performed in triplicate.

Detection of BX1 protein by transmission electron microscopy

Segments of RDC, R2W, and L2W were fixed in 2% (w/v) paraformaldehyde (Sigma-Aldrich, St. Louis, MO, USA) and 2% (w/w) glutaraldehyde (Sigma-Aldrich) in 10 mM phosphate-buffered saline (PBS) buffer pH 7.4 for 2 h. Samples were dehydrated with increasing concentrations of ethanol, and then infiltrated and embedded in epoxy resin (Sigma-Aldrich; equivalent to Epon 812) according to the manufacturer's instructions. The specimens were polymerised at 56°C for 3 days (Brorson et al., 1999). Immunogold labelling for transmission electron microscopy analyses was conducted on sections obtained from the same samples (collected in three independent experiments and at least five randomly selected specimens) using the same 3-µm thick sections examined by light microscopy. Ultrathin sections (90 nm) were made for transmission electron microscopy with a Leica UCT ultramicrotome (Leica Microsystems, Wetzlar, Germany) and placed on nickel grids. Immunogold labelling was performed on grid-mounted thin sections floating in drops, according to Brorson et al., (1999), with modifications. First, ultrathin epoxy sections were treated with 15% H_2O_2 for 10 min, and then rinsed three times for 5 min in MQ water and pre-incubated in 10 mM PBS for 10 min. Sections were incubated in 4% (w/v) BSA diluted in 10 mM PBS (pH 7.2) for 2 h before immunolabeling to block non-specific labelling. The primary purified polyclonal antibody (rabbit Anti-IGPPL, Agrisera) described above was diluted 1:50 in 4% (w/v) BSA and then incubated with the grids 1.5 h at room temperature. Samples were washed in 10 mM PBS with 0.05% (v/v) Tween 20 four times for 10 min and once in 10 mM PBS for 10 min. The secondary antibody (goat anti rabbit conjugated to 18 nm colloidal gold; Jackson ImmunoResearch, Ely, UK) was diluted 1:100 in 4% (w/v) BSA and incubated with the grids for 1 h at room temperature. The grids were then washed three times in 10 mM PBS

with 0.05% (v/v) Tween 20 and rinsed five times in MQ water. The grids were stained with 1.2% (w/v) uranyl acetate solution in 70% methanol (Sigma-Aldrich) for 1 min and washed five times with MQ water, each for 2 min. In negative controls, primary antibody was omitted. Samples were examined under an FEI 268D "Morgagni" (FEI Company, Hillsboro, OR, USA) transmission electron microscope operating at 80 kV. Images were acquired with an SIS "Morada" digital camera (Olympus-SIS, Münster, Germany).

Results

1. *ScBx1* gene expression

Transcripts of *ScBx1* were detected in all analysed organs and organoids. In case of RDC, the transcript level of *ScBx1* was two times lower than that in R2W and 49.8 times lower than that in L2W. In RIV, the transcript level of *ScBx1* was seven times lower than that in RDC, 14 times lower than that in R2W, and nearly 350 times lower than that in L2W (Fig. 1, Table S1; supplementary materials).

Figure 1. Relative transcript levels of *ScBx1* in (a) roots developed from seeds deprived of coleoptile 2 days after sowing (RDC), roots (R2W) and leaves (L2W) of 2-week-old seedlings; (b) roots developed *in vitro* (RIV) of rye inbred line L318. Data are mean ± SD of three biological replicates.

2. BX content

Six BXs were detected in RDC. Two of the six analysed BXs (HBOA and especially DIBOA) were present at higher levels in RDC than in R2W; 1.56 and 2.18 times, respectively. Among all the organs compared, RDC had the highest DIMBOA content. The two other BXs – GDIBOA and GDIMBOA, were detected at lower levels in RDC than in R2W. The GDIMBOA level was 3.36 times higher in RDC than in L2W, and the GDIBOA level was 35.8 times lower in RDC than in L2W. The MBOA content was similar in RDC and R2W, but was nearly 10 times higher in those organs than in L2W (Fig. 2, Table S2; supplementary materials). The total BXs content was lower in RIV than in the other tested organs. GDIMBOA was either not produced in RIV, or its level was beneath the limit of detection. Among the BXs detected in RIV, GDIBOA and DIMBOA were the most abundant, with the DIMBOA content comparable to that in L2W.

Figure 2. Concentrations of benzoxazinoids (BXs) in roots developed from (a) seeds deprived of coleoptile 2 days after sowing (RDC), roots (R2W) and leaves (L2W) of 2-week-old seedlings; and (b) roots developed *in vitro* (RIV) of rye inbred line L318. Data mean ± SD of three biological replicates.

3. Bioinformatics characterisation of BX1 protein

The coding sequence of BX1 was 960 bp long, and encoded a protein of 319 amino acids with a calculated molecular weight of 33.7 kDa. The TargetP 2.0 program (Armenteros et al., 2019) predicted a chloroplast transit peptide of 41 amino acids at the N-terminus, indicating that the mature protein was approximately 29.3 kDa (Fig. 3). The GRAVY index score of BX1 measured by the Kyte-Doolittle formula was above 0, suggesting that the protein may be hydrophobic and membrane-localised.

Database searches revealed that BX1 shared the highest identity (about 97%) with indole-3-glycerol phosphate lyases from *Triticum aeastivum* (Acc. No. KAF7049523), *Triticum turgidum* (Acc. No. VAI07221), and *Aegilops tauschii* (Acc. No. XP_020172362) (Fig. 3), and lower identity with proteins from *Zea mays* (89%), *Sorghum bicolor* (75%), *Digitaria exilis* (73%), *Oryza sativa* (72%), and *Secale cereale* (64%) (Acc. No. NP_001105219, XP_002463738, CAB3497862, XP_015633113, and QIB84921, respectively). The most divergent sequences were found within and after the putative chloroplast transit peptide.

Figure 3. Amino acid sequence alignment of BX1 and other lyases from *Triticum aestivum* (Acc. No. KAF7049523), *Triticum turgidum* (Acc. No. VAI07221), *Aegilops tauschii* (Acc. No. XP_020172362), *Zea Mays* (Acc. No. NP_001105219) *Sorghum bicolor* (Acc. No. XP_002463738), *Digitaria exilis* (Acc. No. CAB3497862), *Oryza sativa* (Acc. No. XP_015633113), and *Secale cereale* (Acc. No. QIB84921). Residues identical between BX1 and all other proteins are shaded. Putative chloroplast transit peptides of proteins as predicted by the TargetP 2.0 are underlined.

4. Immunodetection of BX1 in the plastid fraction of roots

First, the specificity of the affinity-purified anti-BX1 antibodies was determined in western blotting analyses using total proteins extracted from roots of 2-week-old plants. The lack of any protein band indicated that BX1 was not present or its amount was below the limit of detection (Fig. 4a).

Next, the plastids fractions isolated from RDC, R2W and L2W were subjected to immunoblot analyses, which revealed a major band in the membrane fraction and a small band at approximately 29 kDa in the soluble fraction of plastids (Fig. 4a.). No signal was detected in the same protein extracts using pre-immune serum (Fig. 4a). The molecular weight of the protein was highly consistent with the molecular weight calculated from the deduced amino acid sequence.

Relatively larger amounts of BX1 were detected in root plastids, from both RDC (especially) and R2W, than in leaf chloroplasts (Fig. 4b). No signal was detected in the cytosolic fractions of any analysed organs.

The relative purity of isolated plastids and cytosol fractions was verified using compartment marker antibodies directed against FNR and UGpase (Fig. 4b), respectively, and by light microscopy (Fig S2a,b; supplementary materials).

Figure 4. Immunoblot analysis of BX1 in different extracts of roots developed from seeds deprived of coleoptile 2 days after sowing (RDC), roots (R2W) and leaves (L2W) of 2-week-old seedlings from of rye inbred line L318.

- a. Immunospecificity of affinity-purified anti-BX1 polyclonal antibodies in root protein extracts (RDC):

  (1,4) Total proteins from roots

  (2,5) Soluble proteins from root plastids

  (3,6) Membrane proteins from root plastids

  (M) Molecular weight marker (Eurx, Poland)

- b. Detection of BX1 in plastid and cytosol fractions of different organs:

  1. Total fraction of plastids isolated from roots developed from seeds deprived of coleoptile 2 days after sowing (RDC)

  2. Total fraction of plastids isolated from roots of 2-week-old seedlings (R2W)

  3. Total fraction of chloroplasts isolated from leaves of 2-week-old seedlings (L2W)

  4. Cytosolic fraction isolated from RDC

  5. Cytosolic fraction isolated from R2W

  6. Cytosolic fraction isolated from L2W

Sera raised against UDP-glucose pyrophosphorylase (UGPase) (cytosol marker) and ferredoxin NADP reductase FNR (plastid marker) were used in western blots to confirm quality of isolated fractions.

5. Immunolocalisation of BX1 protein in plastids of roots and leaves

To complement the cell fractionation results described above, we conducted immunogold labelling and observed the localisation of labelled components by transmission electron microscopy. The detection of BX1 on an ultrastructural level confirmed its specific localisation in plastids of RDC (Fig. 5) as well as in both controls - plastids of R2W and chloroplasts of L2W (Fig. S3; supplementary materials).

Figure 5. Localisation of BX1 by immunogold labelling and transmission microscopy in roots developed from seeds deprived of coleoptile 2 days after sowing (RDC) of rye inbred line L318. Abbreviations: CW- cell wall, ER- endoplasmic reticulum, M- mitochondrion, Pl- plastid, V- vacuole. Scale bars = 1 µm.

Discussion

Many studies on different aspects BX biosynthesis over the past 50 years have reported that this class of metabolites is present in roots, root exudates, or root extracts of such species as maize (Neal et al., 2012, Neal and Ton 2013, Handrick et al., 2016; Cotton et al., 2019), common wheat (Pérez and Ormenoñuñez 1991, Belz and Hurle 2005, Stochmal et al., 2006, Villagrasa et al., 2006), emmer

10

wheat (Ben-Abu et al., 2018), and rye (Pérez and Ormenoñuñez 1991, Zasada et al., 2007, Schulz et al., 2013, Rakoczy-Trojanowska et al., 2018a, b; Rakoczy-Trojanowska et al., 2020). Also, transcripts of *Bx1*, the first gene controlling the BX biosynthesis pathway, have been detected in roots of rye (Tanwir et al., 2017, Rakoczy-Trojanowska et al., 2018a, b, 2020), wheat (Nomura et. al., 2005), and maize (von Rad et al., 2001, van Doan et al., 2020).

Recently, we proved that a different gene, *ScIgl*, controls the first step of BX biosynthesis at later developmental stages (Wlazło et al., 2020) and that this gene is expressed in roots of rye (Rakoczy-Trojanowska et al., 2020). The results of qRT-PCR analyses of *ScIgl*, which showed the highest transcript levels in RDC and R2W, are presented in Table S1 (supplementary materials).

According to current opinion, the first step in BX biosynthesis, i.e., the conversion of indole-3-glycerol phosphate to indole by BX1, occurs in the aerial parts of plants, specifically – in chloroplasts. Some authors, e.g., Tanwir et al., (2017), have postulated that BXs are mainly biosynthesised in rye shoots, not in roots, and then transported to the roots where they accumulate as methoxylated glycosylated forms. This point of view is difficult to reconcile with the fact that *ScBx1* (as well as its "cooperator", *ScIgl*) is expressed in roots at low but still detectable levels, regardless of cultivation conditions and the plant age and genotype (Rakoczy-Trojanowska et al., 2020). At the same time, the detection of *ScBx1* transcripts and BXs in roots was convincing, but not unequivocal, evidence that the first stage of BX biosynthesis may occur in both aerial parts and roots of rye. Therefore, in this study, we aimed to obtain definitive evidence to show that BX1 is present and active in the roots of rye. This evidence was obtained by performing biochemical, gene expression, and immunological assays of "independent roots" i.e., those developed from seeds deprived of the coleoptile immediately after emergence, so that they had no contact with the photosynthesising aerial plant parts. To provide irrefutable evidence showing that the biosynthesis of BXs can initiate and continue independently in the roots, we conducted gene expression and biochemical analyses of roots developed *in vitro*. These organoids have never come into contact with aerial parts, so we could be sure that any BXs detected in the roots had not been transported from the aerial plants.

To date, no previous studies have focused on the course of BX biosynthesis in rye roots, because the main focus has been on metabolites secreted by roots and their influence on nematodes (Zasada et al., 2007, Meyer et al., 2009, Rice et al., 2012) and weeds (Tabaglio et al., 2008, Gavazzi et al., 2010, Schulz et al., 2013). To the best of our knowledge, no studies have focused on BX biosynthesis in the roots of other species that produce BXs, either.

We detected *ScBx1* transcripts in all four analysed organs – RDC, RIV, R2W, and L2W. As expected, the transcript levels were much lower in roots, particularly RIV, than in leaves of 2-week-old seedlings. Relatively lower transcript levels of *ScBx1* in roots than in aerial parts at early developmental stages (48 h, 72 h, 2 days, 6 days, and 8 days after seed germination) were also reported by Tanwir et al., (2017). The same phenomenon, regardless of cultivation conditions (with or

without Berseem clover), was observed by Rakoczy-Trojanowska et al., (2020). However, the differences in *ScBx1* transcript levels between RDC with R2W were minor.

We detected BXs in almost all analysed tissues (except for GDIMBOA in RIV), with the lowest levels detected in RIV. As expected from the organ-specific nature of BX biosynthesis, the contents of methoxylated BX metabolites (MBOA, DIMBOA, and GDIMBOA) were higher in roots (both RDC and R2W) than in leaves (L2W), whereas the contents of non-methoxylated BX metabolites were higher in leaves than in roots. The same pattern of distribution was detected by Tanwir et al., (2017) and Rakoczy-Trojanowska et al., (2020). In the latter study, the distribution pattern was the same in rye plants cultivated with and without Berseem clover.

Interestingly, in the present study, the concentrations of DIBOA and DIMBOA, two key BXs in rye, were more than two times higher, and that of HBOA was more than 1.5 times higher, in RDC than in R2W. These high concentrations may be because they could not be transported to the aerial parts. During typical plant development, different compounds, including BXs, are transported *via* the xylem from roots to the upper parts (Givovich et al., 1994, Kataoka et al., 2004, Shimpei et al., 2009, Ko et al., 2014). Recently, Hazrati et al., (2020) showed that two BXs, GDIBOA and GDIMBOA, were secreted by rye roots into the soil and then absorbed by the roots of the co-cultivated hairy vetch plants and translocated to their shoots. However, when the contact between roots and upper parts is broken, e.g., by removal of the coleoptiles, metabolites cannot be transported and so they accumulate in excessive amounts at the site of their synthesis, in this case, in the roots. In addition, the pool of BXs in RDC may have increased in response to wounding during coleoptile removal, a factor that has been shown to stimulate BX production (La Hovary 2011). The contents of five out of six BXs were lower in RIV than in the other tested organs; as much as seven times lower than in RDC. The other BX, GDIMBOA, was undetectable rather than absent (because GDIBOA was detected). Plant tissues, especially callus and roots, are capable of producing secondary metabolites (Espinosa-Leal et al., 2018, Ochoa-Villarreal et al., 2016). Therefore, we expected that the concentrations of BXs in RIV would be relatively high. The fact that we detected lower contents of most BXs in RIV than in other organs may be due to the *in vitro* culture conditions; that is, those that induce rhizogenesis, rather than those that induce BX production.

Tanwir et al., (2017) postulated that non-methoxylated BXs (HBOA and DIBOA) were transported to the roots even before removing the coleoptiles. However, this is contradicted by our findings that the contents of both non-methoxylated BXs were higher in RDC than in R2W at a similar stage of development (1.6 times and 2.2 times higher for HBOA and DIBOA, respectively). If the BXs produced in coleoptiles were transported to roots, then the amount would be very small: firstly, because of the early developmental stage (BX synthesis is low in coleoptiles during the first 2 days); secondly, because of the very short contact time between shoots and roots (thus, a short time available for BX transport); and thirdly, because of the long time between removing the coleoptiles and the

sampling time. This possibility is obviously completely excluded in the case of RIV (roots regenerated *in vitro*).

Both immunoassays used in our study detected BX1 in plastids of the roots, including RDC, and in the leaves. Although other studies have detected *Bx1* transcripts in roots, there are no previous reports on the presence and the role of BX1 protein in root plastids. In this study, we report a new observation that has not been previously reported for other lyases. BX1 catalysing indole production has a signal peptide for plastid import, encoded by the first exon of its encoding gene (Gierl and Frey 2001, Zhuang et al., 2011), so its plastid subcellular localisation was expected. Interestingly, we detected the highest levels of BX1 protein in RDC, medium levels in R2W, and the lowest levels in L2W, opposite to the trends in *ScBx1* transcript levels. A poor correlation between mRNA levels and protein levels in eukaryotes, where the two processes are spatially separated, is a well-known phenomenon that has been reported by many authors (for reviews see: Vélez-Bermúdez and Schmidt 2014, Liu et al., 2016, Sablok et al., 2017). It can be assumed that in RDC, which develop under conditions of permanent stress, a limited amount of mRNA is used more effectively than are the larger amounts of mRNA in the other two organs. Upon environmental challenges, e.g., in roots developing atypically without contact with photosynthesising upper plant parts, translation would be regulated to reduce energy consumption, as noted by Echevarría-Zomeño et al., (2013). All this might imply a highly efficient enzymatic reaction of the conversion of indole to indolin-1-one in RDC. Moreover, the course and specificity of post-transcriptional regulatory processes (e.g. formation of alternative splicing variants resulting from intron retention and alternative $5'$ and $3'$ splice sites; Li at al., 2013) may explain the weak relationship between the observed transcript and protein levels. Our results highlight that transcriptomic data should be interpreted with caution and should not be the basis for far-reaching conclusions.

The presence of BX1 in RDC, R2W, and L2W is further evidence that BX biosynthesis can occur independently in roots and leaves. Moreover, the higher levels of BX1 protein in R2W and especially in RDC indicate high efficiency of the enzymatic reaction in roots (particularly in roots developing independently without contact with photosynthesising upper plant parts).

On the basis of the results of all our analyses, that is, the detectable transcript levels of *ScBx1*, high contents of three BXs (HBOA, DIBOA and DIMBOA), and large amounts of BX1 protein in RDC and RIV, we conclude that BXs are synthesised *de novo* in roots, independently of aerial plant parts. Our results do not exclude the possibility that some BXs are transported from the aerial parts to the roots. Therefore, we would like to update the currently accepted opinion that the first stage occurs only in chloroplasts; on the contrary, it can also take place in roots, at least in rye. Our results not only broaden knowledge of BX biosynthesis but also may have potential practical applications. The fact that BXs (including those that function in defence, such as DIBOA and DIMBOA) are synthesised in roots without contact with the aerial parts, especially roots regenerated *in vitro*, opens opportunities to produce these compounds in roots and, very likely, in hairy root *in vitro* cultures. This will require the

development of appropriate methodologies including appropriate stimulators, media, internal and external *in vitro* culture conditions, and biotic and abiotic elicitors, as suggested by Espinosa-Leal et al., (2018) and Chandran et al., (2020), among others.

Supplementary materials

Fig. S1. Twelve-day-old roots developed from seeds deprived of coleoptile; rye inbred line L318.

Table S1. Relative transcript levels of *ScBx1* and *ScIgl* in rye roots developed from seeds deprived of coleoptile 2 days after germination (RDC), root primordia developed *in vitro* (RIV), roots (R2W) and leaves (L2W) of 2-week-old seedlings.

Table S2. Contents of six benzoxazinoids in roots developed from RDC, RIV, R2W and L2W of 2-week-old seedlings of rye inbred line L318.

Fig. S2. Plastids isolated from roots developed from (a) seeds deprived of coleoptile at 2 days after sowing and (b) leaves of 2-week-old seedlings of rye inbred line L318.

Fig. S3. Localisation of indole-3-glycerol phosphate lyase by immunogold labelling and transmission microscopy in R2W and L2W of 2-week-old seedlings of rye inbred line L318.

Acknowledgements

Author contributions

M.R-T designed and supervised the experiments, wrote the manuscript; E.R. and B.Ł. – performed microscope immunolocalisation of BX1; M.′S. and B.B. - performed the expressional analyses; W.B. – designed and performed in vitro experiments; M.K. - conducted biochemical analysis. B.S. designed and performed immunodetection of BX1, and bioiformatical analysis of BX1. All authors have read and approved the final manuscript.

Data availability All data supporting the findings of this study are available within the paper and within its supplementary materials published online.

References

Armenteros JJA, Salvatore M, Emanuelsson O, Winther O, von Heijne G, Elofsson A, Nielsen H. 2019. Detecting sequence signals in targeting peptides using deep learning. Life Science Alliance 2(5):e201900429. https://doi.org/10.26508/lsa.201900429

Bakera B, Makowska B, Groszyk J, Niziołek M, Orczyk W, Bolibok-Brągoszewska H, Hromada-Judycka A, Rakoczy-Trojanowska M. 2016. Structural characteristics of *ScBx* genes controlling the biosynthesis of hydroxamic acids in rye (*Secale cereale* L.). Journal of Applied Genetics 57:285. https://doi.org/10.1007/s13353-016-0342-9

Belz RG, Hurle K. 2005. Differential exudation of two benzoxazinoids—one of the determining factors for seedling allelopathy of Triticeae species. Journal of Agricultural and Food Chemistry 53(2):250–261. https://doi.org/10.1021/jf048434r

Ben-Abu Y, Beiles A, Flom D, Nevo E. 2018. Adaptive evolution of benzoxazinoids in wild emmer wheat, *Triticum dicoccoides*, at "EvolutionCanyon", MountCarmel, Israel. PLoS One 13(2):e0190424. https://doi.org/10.1371/journal.,pone.0190424

Brorson S-H, Hansen AR, Nielsen HZ, Woxen IK. 1999. A comparative study of the immunogold labelling on H2O2- treated and heated epoxy sections. Micron 32(2):147-151. https://doi.org/10.1016/S0968-4328(99)00107-9

Chandran H, Meena M, Barupal T, Sharma K. 2020. Plant tissue culture as a perpetual source for production of industrially important bioactive compounds. Biotechnology reports (Amsterdam, Netherlands) 26: e00450. https://doi.org/10.1016/j.btre.2020.e00450.

Cotton TEA, Pétriacq P, Cameron DD, Meselmani MA, Schwarzenbacher R, Rolfe SA, Tin J. 2019. Metabolic regulation of the maize rhizobiome by benzoxazinoids. ISME Journal 13:1647–1658. https://doi.org/10.1038/s41396-019-0375-2

Echevarría-Zomeño S, Yángüez E, Fernández-Bautista N, Castro-Sanz AB, Ferrando A, Castellano MM. 2013. Regulation of translation initiation under biotic and abiotic stresses. International Journal of Molecular Sciences 14(3):4670-4683. https://doi.org/10.3390/ijms14034670

Espinosa-Leal CA, Puente-Garza CA, García-Lara S. 2018. *In vitro* plant tissue culture: means for production of biological active compounds. Planta 248:1–18. https://doi.org/10.1007/s00425-018-2910-1

Frey M, Schullehner K, Dick R, Fiesselmann A, Gierl A. 2009. Benzoxazinoid biosynthesis, a model for evolution of secondary metabolic pathways in plants. Phytochemistry 70(15-16):1645–1651. https://doi.org/10.1016/j.phytochem.2009.05.012

Frey M, Stettner C, Pare PW, Schmelz EA, Tumlinson JH, Gierl A. 2000. An herbivore elicitor activates the gene for indole emission in maize. Proceedings of the National Academy of Sciences of U S A. 97(26):14801-14806. https://doi.org/10.1073/pnas.260499897

Frey M, Chomet P, Glawischnig E, *et al*. 1997. Analysis of a chemical plant defense mechanism in grasses. Science 277(5326):696-699. https://doi.org/10.1126/science.277.5326.696

Gavazzi C, Schulz M, Marocco A, Tabaglio V. 2010. Sustainable weed control by allelochemicals from rye cover crops: from the greenhouse to field evidence. Allelopathy Journal 25:259–273.

Gierl A, Frey M. 2001. Evolution of benzoxazinone biosynthesis and indole production in maize. Planta 213(4):493–498. https://doi.org/10.1007/s004250100594

Givovich A, Sandström J, Niemeyer HM, Pettersson J. 1994. Presence of a hydroxamic acid glucoside in wheat phloem sap, and its consequences for performance of *Rhopalosiphum padi* (L.) (*Homoptera: Aphididae*). Journal of Chemical Ecology 20(8):1923-1930. https://doi.org/10.1007/BF02066233

Handrick V, Robert CAM, Ahern KR, *et al.* 2016. Biosynthesis of 8-*O*-methylated benzoxazinoid defence compounds in maize. Plant Cell 28(7):1682-1700. https://doi.org.10.1105/tpc.16.00065

Hazrati H, Fomsgaard IS, Kudsk P. 2020. Root-exuded benzoxazinoids: uptake and translocation in neighboring plants. Journal of Agricultural and Food Chemistry 68(39):10609-10617. https://doi.org/10.1021/acs.jafc.0c04245

Kataoka T, Hayashi N, Yamaya T, Takahashi H. 2004. Root-to-shoot transport of sulfate in arabidopsis. evidence for the role of SULTR3;5 as a component of low-affinity sulfate transport system in the root vasculature. Plant Physiology 136(4):4198-4204. https://doi.org/10.1104/pp.104.045625

Ko D, Kang J, Kiba T, *et al.* 2014. *Arabidopsis* ABCG14 is essential for the root-to-shoot translocation of cytokinin. PNAS 111(19):7150–7155. https://doi.org/10.1073/pnas.1321519111

Kyte J, Doolittle RF. 1982. A simple method for displaying the hydropathic character of a protein. Journal of Molecular Biology 157(1):105-132. https://doi.org/10.1016/0022-2836(82)90515-0

La Hovary C. 2011. Allelochemicals in *Secale cereale*: Biosynthesis and Molecular Biology of Benzoxazinones. Available online: https://repository.lib.ncsu.edu/handle/1840.16/6844 (accessed on 5 May 2020).

Li W, Lin W D, Ray P, Lan P, Schmidt W. 2013. Genome-wide detection of condition-sensitive alternative splicing in *Arabidopsis* roots. Plant Physiology 162(3):1750–1763. https://doi.org/10.1104/pp.113.217778

Liu Y, Beyer A, Aebersold R. 2016. On the dependency of cellular protein levels on mRNA abundance. Cell 165(3):535-550. https://doi.org/10.1016/j.cell.2016.03.014

Livak KJ, Schmittgen TD. 2001. Analysis of relative gene expression data using real-time quantitative PCR and $2^{-\Delta\Delta C_T}$ method. Methods 25(4):402-408. https:/doi.org/10.1006/meth.2001.1262

Makowska B, Bakera B, Rakoczy-Trojanowska M. 2015. The genetic background of benzoxazinoid biosynthesis in cereals. Acta Physiologiae Plantarum 37:176. https://doi.org/10.1007/s11738-015-1927-3

Meihls LN, Handrick V, Glauser G, *et al*. 2013. Natural variation in maize aphid resistance is associated with 2, 4-dihydroxy-7-methoxy-1, 4-benzoxazin-3-one glucoside methyltransferase activity. Plant Cell 25(6):2341-2355. https://doi.org/10.1105/tpc.113.112409

Meyer SLF, Rice CP, Zasada IA. 2009. DIBOA: Fate in soil and effects on root – knot nematode egg numbers. Soil Biology and Biochemistry 41:1555–1560. https://doi.org/10.1016/j.soilbio.2009.04.016

Neal AL, Ahmad S, Gordon-Weeks R, Ton J. 2012. Benzoxazinoids in root exudates of maize attract *Pseudomonas putida* to the rhizosphere. PLoS One 7(4):e35498. https://doi.org/10.1371/journal.,pone.0035498

Neal AL, Ton J. 2013. Systemic defense priming by *Pseudomonas putida* KT2440 in maize depends on benzoxazinoid exudation from the roots. Plant Signaling and Behavior 8(1):e22655. https://doi.org/10.4161/psb.22655

Nomura T, Ishihara A, Yanagita RC, Endo TR, Iwamura H. 2005. Three genomes differentially contribute to the biosynthesis of benzoxazinones in hexaploid wheat. PNAS 102(45):16490–16495. https://doi.org/10.1073/pnas.0505156102

Ochoa-Villarreal M, Howat S, Hong S, Jang MO, Jin YW, Lee EK, Loake GJ. 2016. Plant cell culture strategies for the production of natural products. BMB Reports 49:149–158. https://doi.org/10.5483/BMBRep.2016.49.3.264

Pérez FJ, Ormenoñuñez J. 1991. Difference in hydroxamic acid content in roots and root exudates of wheat (*Triticum aestivum* L.) and rye (*Secale cereale* L.): Possible role in allelopathy. Journal of Chemical Ecology 17:1037–1043. https://doi.org/10.1007/BF01402932

Rakoczy-Trojanowska M, Święcicka M, Bakera B, Kowalczyk M, Stochmal A, Bolibok L. 2020. Co-cultivating rye with berseem clover affects benzoxazinoid production and expression of related genes. Crop Science 60(6):3228-3246. https://doi.org/10.1002/csc2.20263

Rakoczy-Trojanowska M, Święcicka M, Rymuszka J, Stochmal A, Kowalczyk M. 2018a. New aspects of the genetic background of benzoxazinoid biosynthesis in rye *Secale cereale* L. EUCARPIA cereal section / IWIW2 meetings, March 19-22, 2018. Polydôme, Clermont-Ferrand, France: PI-23

Rakoczy-Trojanowska M, Święcicka M, Bakera B, Wlazło A. 2018b. Genetic and environmental determinants regulating benzoxazinoid biosynthesis in rye (*Secale cereale* L) - facts and myths. Integrative Plant Biology Conference, IPG PAS 7 th – 9 th November 2018. Poznan, Poland: 71

Rice CP, Cai G, Teasdale JR. 2012. Concentrations and allelopathic effects of benzoxazinoid compounds in soil treated with rye (*Secale cereale*) cover crop. Journal of Agricultural and Food Chemistry 60(18):4471–4479. https://doi.org/10.1021/jf300431r

Rice CP, Park YB, Adam F, Abdul-Baki AA, Teasdale JR. 2005. Hydroxamic acid content and toxicity of rye at selected growth stages. Journal of Chemical Ecology 31(8):1887-1905. https://doi.org/10.1007/s10886-005-5933-6

Sablok G, Powell JJ, Kazan K. 2017. Emerging Roles and Landscape of Translating mRNAs in Plants. Frontiers in Plant Science 8:1443. https://doi.org/10.3389/fpls.2017.01443

Schulz M, Marocco A, Tabaglio V, Macías F, Molinillo J. 2013. Benzoxazinoids in rye allelopathy - from discovery to application in sustainable weed control and organic farming. Journal of Chemical Ecology 39(2):154-174. https://doi.org/10.1007/s10886-013-0235-x.

Shimpei U, Shinsuke M, Masato K, Akira K, Tomohito A, Satoru I. 2009. Root-to-shoot Cd translocation via the xylem is the major process determining shoot and grain cadmium accumulation in rice. Journal of Experimental Botany 60(9):2677-2688. https://doi.org/10.1093/jxb/erp119

Stochmal A, Kus J, Martyniuk S, Oleszek W. 2006. Concentration of benzoxazinoids in roots of field-grown wheat (*Triticum aestivum* L.) varieties. Journal of Agricultural and Food Chemistry 54(4):1016-1022. https://doi.org/10.1021/jf050899

Święcicka M, Dmochowska-Boguta M, Orczyk W, Grądzielewska A, Stochmal A, Kowalczyk M, Bolibok L, Rakoczy-Trojanowska M. 2020. Changes in benzoxazinoid contents and the expression of the associated genes in rye (*Secale cereale* L.) due to brown rust and the inoculation procedure. PLoS One 15(5):e0233807. https://doi.org/10.1371/journal.,pone.0233807.

Tabaglio V, Gavazzi C, Schulz M, Marocco A. 2008. Alternative weed control using the allelopathic effect of natural benzoxazinoids from rye mulch. Agronomy for Sustainable Development 28:397–401. hal-00886420

Tanwir F, Dionisio G, Adhikari KB, Fomsgaard IS, Gregersen PL. 2017. Biosynthesis and chemical transformation of benzoxazinoids in rye during seed germination and the identification of a rye *Bx6*-like gene. Phytochemistry 140:95-107. https://doi.org/10.1016/j.phytochem.2017.04.020

Van Doan C, Züst T, Maurer C, Zhang X, Machado RAR, Mateo P, Ye M, Schimmel BCJ, Glauser G, Robert CAM. 2020. Tissue-specific volatile-mediated defense regulation in maize leaves and roots. bioRxiv. https://doi.org/10.1101/2020.02.21.959437.

Vélez-Bermúdez IC, Schmidt W. 2014. The conundrum of discordant protein and mRNA expression. Are plants special? Frontiers in Plant Science 5:616. https://doi.org/10.3389/fpls.2014.00619

Villagrasa M, Guillamón M, Labandeira A, Taberner A, Eljarrat E, Barceló D. 2006. Benzoxazinoid allelochemicals in wheat: distribution among foliage, roots, and seeds. Journal of Agricultural and Food Chemistry 54(4):1009-1015. DOI: 10.1021/jf050898h

Von Rad U, Huttl R, Lottspeich F, Gierl A, Frey M. 2001. Two glucosyltransferases are involved in detoxification of benzoxazinoids in maize. Plant Journal 28(6):633–642. https://doi.org/10.1046/j.1365-313x.2001.01161.x

Wang CS, Jiang QT, Ma J, Wang XY, Wang JR, Chen GY, Qi PF, Pen YY, Lan XJ, Zheng YL, Wei YM. 2016. Characterization and expression analyses of the H+-pyrophosphatase gene in rye. Journal of Genetics 95:565-572. https://doi.org/10.1007/s12041-016-0664-8

Wlazło A, Święcicka M, Koter MD, Krępski T, Bolibok L, Stochmal A, Kowalczyk M, Rakoczy-Trojanowska M. 2020. Genes *ScBx1* and *ScIgl*–Competitors or Cooperators? Genes 11(2):223. https://doi.org/10.3390/genes11020223

Wouters FC, Blanchett B, Gershenzo J, Vassão DG. 2016. Plant defense and herbivore counter-defense: benzoxazinoids and insect herbivores. Phytochemistry Reviews 15(6):1127-1151. https://doi.org/10.1007/s11101-016-9481-1

Zasada IA, Rice CP, Meyer SLF. 2007. Improving the use of rye (*Secale cereale*) for nematode management: potential to select cultivars based on *Meloidogyne incognita* host status and benzoxazinoid content. Nematology 9(1):53–60. https://doi.org/10.1163/156854107779969745

Zhuang X, Fiesselmannb A, Zhaoa N, Chena H, Monika Frey M, Chen F. 2011. Biosynthesis and emission of insect herbivory-induced volatile indole in rice. Phytochemistry 73:15-22. https://doi.org/10.1016/j.phytochem.2011.08.029

Tables

Table 1. Primers used in the qRT-PCR reactions.

Gene	Sequences (5′–3′)
ScBx1	F: TCAAAACCTGAACACGTGAAGC
	R: GCCTCTAGCCTTTTCAATCCTTC
HvAct	F: CCCCTTTGAACCCAAAAGCC
	R: GAAAGCACGGCCTGAATAGC

Figure legends

Figure 1. Relative transcript levels of *ScBx1* in (a) roots developed from seeds deprived of coleoptile 2 days after sowing (RDC), roots (R2W) and leaves (L2W) of 2-week-old seedlings; (b) roots developed *in vitro* (RIV) of rye inbred line L318. Data are mean ± SD of three biological replicates.

Figure 2. Concentrations of benzoxazinoids (BXs) in roots developed from (a) seeds deprived of coleoptile 2 days after sowing (RDC), roots (R2W) and leaves (L2W) of 2-week-old seedlings; and (b) roots developed *in vitro* (RIV) of rye inbred line L318. Data mean ± SD of three biological replicates.

Figure 3. Amino acid sequence alignment of BX1 and other lyases from *Triticum aestivum* (Acc. No. KAF7049523), *Triticum turgidum* (Acc. No. VAI07221), *Aegilops tauschii* (Acc. No. XP_020172362), *Zea Mays* (Acc. No. NP_001105219) *Sorghum bicolor* (Acc. No. XP_002463738), *Digitaria exilis* (Acc. No. CAB3497862), *Oryza sativa* (Acc. No. XP_015633113), and *Secale cereale* (Acc. No. QIB84921). Residues identical between BX1 and all other proteins are shaded. Putative chloroplast transit peptides of proteins as predicted by the TargetP 2.0 are underlined.

Figure 4. Immunoblot analysis of BX1 in different extracts of roots developed from seeds deprived of coleoptile 2 days after sowing (RDC), roots (R2W) and leaves (L2W) of 2-week-old seedlings from of rye inbred line L318.

    a. Immunospecificity of affinity-purified anti-BX1 polyclonal antibodies in root protein extracts (RDC):

        (1,4) Total proteins from roots

        (2,5) Soluble proteins from root plastids

        (3,6) Membrane proteins from root plastids

        (M) Molecular weight marker (Eurx, Poland)

    b. Detection of BX1 in plastid and cytosol fractions of different organs:

        1. Total fraction of plastids isolated from roots developed from seeds deprived of coleoptile 2 days after sowing (RDC)

        2. Total fraction of plastids isolated from roots of 2-week-old seedlings (R2W)

20

3. Total fraction of chloroplasts isolated from leaves of 2-week-old seedlings (L2W)

4. Cytosolic fraction isolated from RDC

5. Cytosolic fraction isolated from R2W

6. Cytosolic fraction isolated from L2W

Sera raised against UDP-glucose pyrophosphorylase (UGPase) (cytosol marker) and ferredoxin NADP reductase FNR (plastid marker) were used in western blots to confirm quality of isolated fractions.

Figure 5. Localisation of BX1 by immunogold labelling and transmission microscopy in roots developed from seeds deprived of coleoptile 2 days after sowing (RDC) of rye inbred line L318. Abbreviations: CW- cell wall, ER- endoplasmic reticulum, M- mitochondrion, Pl- plastid, V- vacuole. Scale bars = 1 µm.
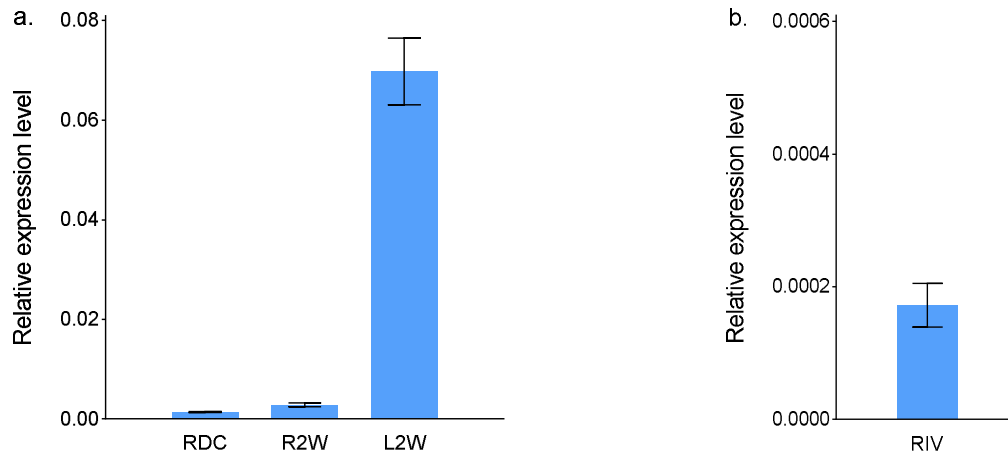
Figures

Figure 1. Relative transcript levels of *ScBx1* in (a) roots developed from seeds deprived of coleoptile 2 days after sowing (RDC), roots (R2W) and leaves (L2W) of 2-week-old seedlings; (b) roots developed *in vitro* (RIV) of rye inbred line L318. Data are mean ± SD of three biological replicates.
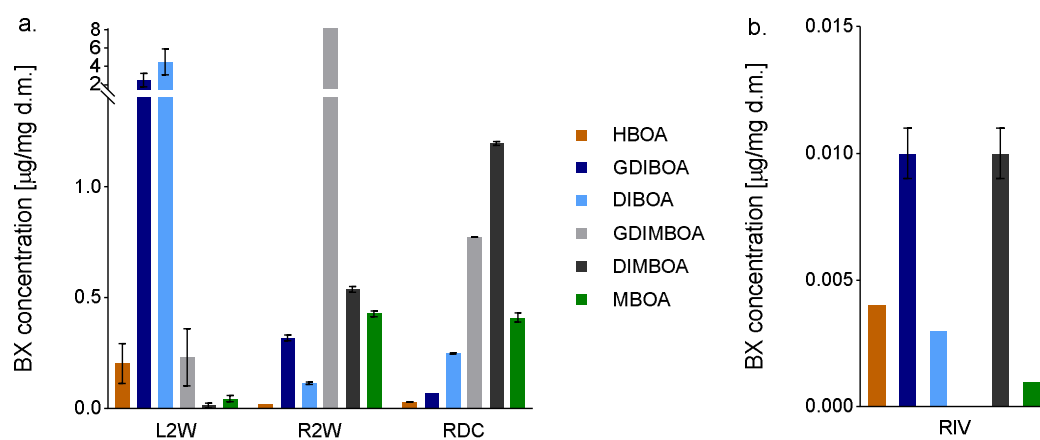
Figure 2. Concentrations of benzoxazinoids (BXs) in roots developed from (a) seeds deprived of coleoptile 2 days after sowing (RDC), roots (R2W) and leaves (L2W) of 2-week-old seedlings; and (b) roots developed *in vitro* (RIV) of rye inbred line L318. Data mean ± SD of three biological replicates.

```
Secale cereale(BX1)   ---------MAFALNASCYPS-------SFQSSLLPRRMAAAVVIPGRRNVLPVIRAV---        42
Triticum aestivum     ---------MAFALNASCYPS-------SFQSSLLPRRMAAAVMIPRRRNVLPVIRAV--         42
Triticum durum        MKVSQSASEMAFALNASCYPS-------SFQSSLLPRRMAAAVMIPRRRNVLPVIRAV---        51
Aegilops tauschii     ---------MAFALNASCYPS-------SF-SSLLPWRMAAAVMIPRRRNVLPVIKAV---        41
Zea mays              ---------MAFAPKTSSSSSLSSALQAAQSPPLLLRRMSST-ATPRRRYDAAVVVTTTTT       51
Sorghum bicolor       ---------MASAIKAASTSRWSSSPA-VQS-SPLPKRV----AMPGRRRSVATVRSVA--       44
Digitaria exilis      ---------MAFALKVASTSQLASSPA-VQSSSPLPRRAAAMATVPRRRKAPAAIRAVA--       49
Oryza sativa          ---------MAFTVKASSPSSPAA----SSSSSSAPAKLG---AAPGRVAVRKLTAA----       41
Secale cereale(IGL)   ---------MAFALKASSLAPSLTHPMRRGTVPA------VAVPAPGRPVVRAVAAA----       42


Secale cereale(BX1)   ----------A---------VAPTAPAPAKPAA-VRSRTVSDTMAKLMAKGKTALIPYITA       83
Triticum aestivum     ----------A---------VAPPALAPAKPAA-VRGRTVSDTMAKLMAKGKTALIPYITA       83
Triticum durum        ----------A---------VAPPALAPAKPAA-VRGRTVSDTMAKLMAKGKTALIPYITA       92
Aegilops tauschii     ----------A---------VAPPAPAPAKPAA-VRSRPVSVTMAKLMAKGKTALIPYITA       82
Zea mays              ARAAAAAVTVPAAPPQAPAPAPVPPKQAAAPAE-RRSRPVSDTMAALMAKGKTAFIPYITA      110
Sorghum bicolor       -----------------AV-APAAP--APARLT-GAGLTVSQTMSKLRAQGKTAFIPYITA       84
Digitaria exilis      -----------------AAVAPAAPLAPAKPAR-KRCLPVSETMSRLMANGKTAFIPYLTA       92
Oryza sativa          ------------------ATSLRLDRAPAAPATERGLSSVSRTMSRLMEKGKTAFIPYITA       84
Secale cereale(IGL)   --------AVASLEPAATVPA---PALAGRSAAGKRGLSVAEAMSRVRANGKTAFIPYITA       92


Secale cereale(BX1)   GDPDLATTAEALRLLDACGADVIELGVPCSDPYVDGPIIQASSARALASGATMDGVLAMLK      143
Triticum aestivum     GDPDLATTAEALRLLDACGADVIELGVPCSDPYVDGPIIQASSARALAGGATMDGVLAMLK      143
Triticum durum        GDPDLATTAEALRLLDACGADVIELGVPCSDPYVDGPIIQASSARALAGGATMDGVLAMLK      152
Aegilops tauschii     GDPDLATTAEALRLLDACGADVIELGVPCSDPYVDGPIIQASSARALAGGATMDGVLAMLK      142
Zea mays              GDPDLATTAEALRLLDGCGADVIELGVPCSDPYIDGPIIQASVARALASGTTMDAVLEMLR      171
Sorghum bicolor       GDPDLATTAEALRLLDACGADVIELGVPFSDPYADGPVIQASAARALASGTTPDAVLAMLQ      144
Digitaria exilis      GDPDLSTTAEALRLLDACGADVIELGVPCSDPYADGPA---STARALAGGVTLDGVLAMLK      148
Oryza sativa          GDPDMGTTAEALRLLDACGADVIELGVPFSDPYNDGPVIQASAARALSAGATMDGIMSMLA      144
Secale cereale(IGL)   GDPDLVTTAEALRLLDSLGADVIELGLPFSDPSADGPVIQASAARALAAGATTDAVMSMLK      152


Secale cereale(BX1)   EVTPELSCPVVLFSYYRPILCRGLAE----IKEAGVHGLIVPDLPYVAAHSLWSEAKKNNL      199
Triticum aestivum     EVTPELSCPVVLFSYYRPILCRGLAE----IK---EAGLIVPDLPYVAAHALWSEAKKNNL      196
Triticum durum        EVTPELSCPVVLFSYYRPILCRGLAE----IKEAGVHGLIVPDLPYVAAHALWSEAKKNNL      208
Aegilops tauschii     EVTPELSCPVVLFSYYRPILCRGLAE----IKEAGVHGLIVPDLPYVAAHSLWSEAKNNNL      198
Zea mays              EVTPELSCPVVLLSYYKPIMSRSLAE----MKEAGVHGLIVPDLPYVAAHSLWSEAKNNNL      227
Sorghum bicolor       EVTPELSCPVVLFSYFNPIVHWGLPDFAAAVKDAGVHGLIVPDLPYGASCALRTEAIKNNI      204
Digitaria exilis      EVTPELSCPVVLFSYFKPIMERGMADFAAAAEEAGVHGLLVPDLPSVATSALRSEAMKNNL      209
Oryza sativa          EVTPELSCPVVLFSYLGPIVRRGPANFTAAAKEAGVQGLIVPDLPYLEACSFRSEVIKNNL      204
Secale cereale(IGL)   EVTPELSCPVVIFSYLSPILRRGTGSFAVAAKEAGVKGLIVPDLPYDQIHAFRKETIMNNL      212


Secale cereale(BX1)   ELVLLTTPAIPEERMKEITKASEGFIYLVSVNGVTGPRENVNLRVESLIQEIKKVTDKPVA      259
Triticum aestivum     ELVLLTTPAIPEERMKEITKASEGFIYLVSVNGVTGPRENVNLRVESLIQEIKKVTDKPVA      256
Triticum durum        ELVLLTTPAIPEERMKEITKASEGFIYLVSVNGVTGPRENVNLRVESLIQEIKKVTDKPVA      268
Aegilops tauschii     ELVLLTTPAIPEERMKEITKASEGFIYLVTVNGVTGPRENVNLRVESLIQEIKKVTDKPVA      258
Zea mays              ELVLLTTPAIPEDRMKEITKASEGFVYLVSVNGVTGPRANVNPRVESLIQEVKKVTNKPVA      287
Sorghum bicolor       ELVLLTTPSTPADRMEEITKASQGFVYLVSVNGVTGPRANVNTRVESLIQEVKQVTDKPVA      264
Digitaria exilis      ELVLLTTPATPEERMREITEASDGFVYLVSVNGVTGPRANVNTRVESLIQEVKQVTDKPVA      269
Oryza sativa          ELVLLTTPTTPPDRMKAITAASGGFVYLVSVNGVTGSRQDVNPRVEHLLQEIKQVTDKAVC      264
Secale cereale(IGL)   ELILLTTPATPSERMKEITNASEGFVYLVSVVGVTGARATVNPRVKDLLQEIRQVTDKAVA      272


Secale cereale(BX1)   VGFGISKPEHVKQIAGWGADGVIIGSAMVRQLGEAASPKEGLKRLEAYARSMKNALP--       319
Triticum aestivum     VGFGISKPEHVKQIAGWGADGVIIGSAMVRQLGEAASPKEGLKRLEAYARSMKNALP--       316
Triticum durum        VGFGISKPEHVKQIAGWGADGVIIGSAMVRQLGEAASPKEGLKRLEAYARSMKNALP--       328
Aegilops tauschii     VGFGISKPEHVKQIARWGADGVIIGSAMVRQLGEAASPREGLKRLEAYARSMKNALP--       318
Zea mays              VGFGISKPEHVKQIAQWGADGVIIGSAMVRQLGEAASPKQGLRRLEEYARGMKNALP--       347
Sorghum bicolor       VGFGISKPEHVKQIAEWGADGVIIGSAMVRQLGEAASPKEGLKRLEKYARSMKNALPCQ      326
Digitaria exilis      VGFGISTPEHVKQIAEWGADGVIIGSAMVRQLGEAASPKEGLRRLEKYARSMKNALP--       329
Oryza sativa          VGYGISTPDHVRQIAEWGADGVIIGSAMVRQLGEAASPKQGLKRLEKYARSLKNALP--       324
Secale cereale(IGL)   VGFGISTPEHVSQIAEWGSDGVIIGSAMVKQLGEANSPREGLKRLEVYAKSLKNALP--       332
```

Figure 3. Amino acid sequence alignment of BX1 and other lyases from *Triticum aestivum* (Acc. No. KAF7049523), *Triticum turgidum* (Acc. No. VAI07221), *Aegilops tauschii* (Acc. No. XP_020172362), *Zea Mays* (Acc. No. NP_001105219) *Sorghum bicolor* (Acc. No. XP_002463738), *Digitaria exilis* (Acc. No. CAB3497862), *Oryza sativa* (Acc. No. XP_015633113), and *Secale cereale* (Acc. No. QIB84921). Residues identical between BX1 and all other proteins are shaded. Putative chloroplast transit peptides of proteins as predicted by the TargetP 2.0 are underlined.
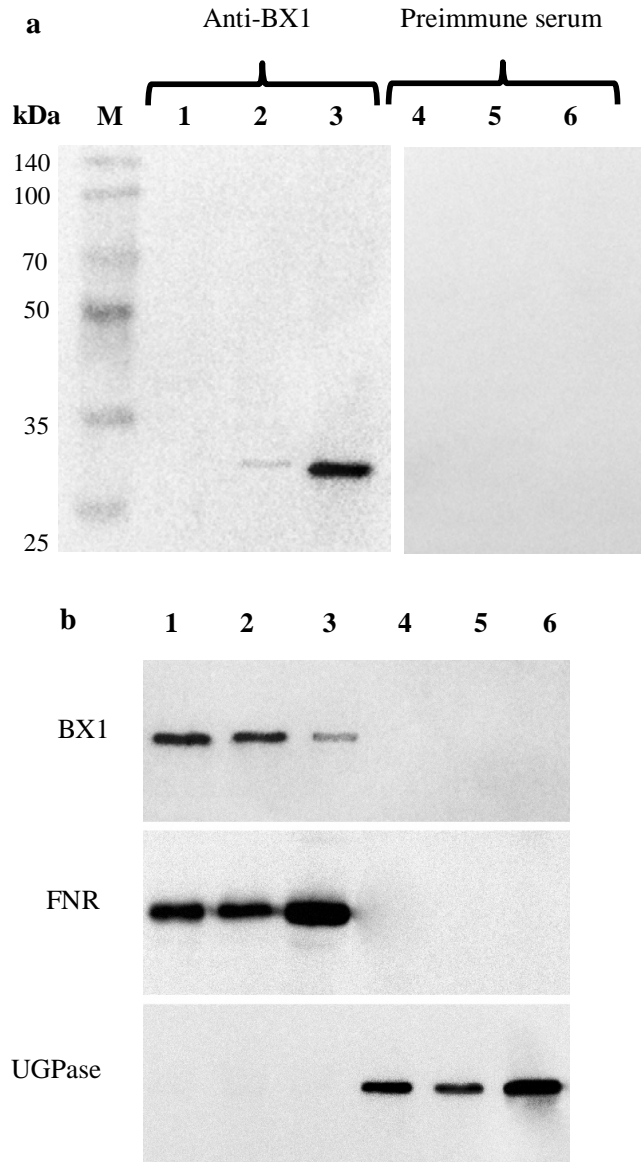
Figure 4. Immunoblot analysis of BX1 in different extracts of roots developed from seeds deprived of coleoptile 2 days after sowing (RDC), roots (R2W) and leaves (L2W) of 2-week-old seedlings from of rye inbred line L318.

    a. Immunospecificity of affinity-purified anti-BX1 polyclonal antibodies in root protein extracts (RDC):

        (1,4) Total proteins from roots

        (2,5) Soluble proteins from root plastids

        (3,6) Membrane proteins from root plastids

        (M) Molecular weight marker (Eurx, Poland)

    b. Detection of BX1 in plastid and cytosol fractions of different organs:

1. Total fraction of plastids isolated from roots developed from seeds deprived of coleoptile 2 days after sowing (RDC)
2. Total fraction of plastids isolated from roots of 2-week-old seedlings (R2W)
3. Total fraction of chloroplasts isolated from leaves of 2-week-old seedlings (L2W)
4. Cytosolic fraction isolated from RDC
5. Cytosolic fraction isolated from R2W
6. Cytosolic fraction isolated from L2W

Sera raised against UDP-glucose pyrophosphorylase (UGPase) (cytosol marker) and ferredoxin NADP reductase FNR (plastid marker) were used in western blots to confirm quality of isolated fractions.
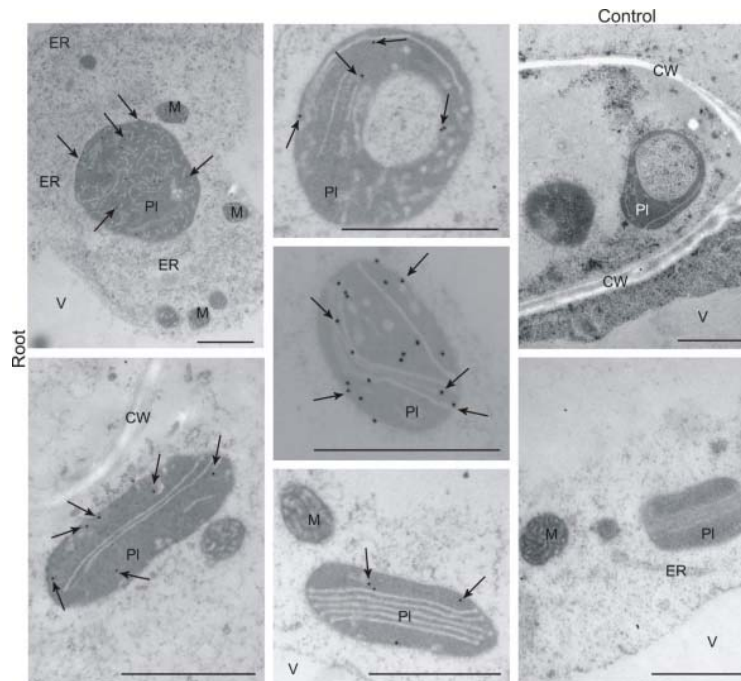
Figure 5. Localisation of BX1 by immunogold labelling and transmission microscopy in roots developed from seeds deprived of coleoptile 2 days after sowing (RDC) of rye inbred line L318. Abbreviations: CW- cell wall, ER- endoplasmic reticulum, M- mitochondrion, Pl- plastid, V- vacuole. Scale bars = 1 µm.